

Title	Renal cortical oxygen tension is decreased following exposure to long-term but not short-term intermittent hypoxia in the rat
Authors	O'Neill, Julie;Jasioneck, Greg;Drummond, Sarah E.;Brett, Orla;Lucking, Eric F.;Abdulla, Mohammed A.;O'Halloran, Ken D.
Publication date	2019-01-16
Original Citation	O'Neill, J., Jasioneck, G., Drummond, S. E., Brett, O., Lucking, E. F., Abdulla, M. A. and O'Halloran, K. D. (2019) 'Renal cortical oxygen tension is decreased following exposure to long-term but not short-term intermittent hypoxia in the rat', American Journal of Physiology - Renal Physiology. doi:10.1152/ajprenal.00254.2018
Type of publication	Article (peer-reviewed)
Link to publisher's version	10.1152/ajprenal.00254.2018
Rights	© 2019, American Journal of Physiology-Renal Physiology. All rights reserved.
Download date	2023-05-07 22:05:49
Item downloaded from	http://hdl.handle.net/10468/7350

Renal Cortical Oxygen Tension is Decreased Following Exposure to Long-term but not Short-term Intermittent Hypoxia in the Rat

Julie O'Neill, Greg Jasionek, Sarah E. Drummond, Orla Brett, Eric F. Lucking, Mohammed A. Abdulla, and Ken D. O'Halloran.

Department of Physiology, School of Medicine, College of Medicine and Health, University College Cork, Cork, Ireland.

Running Title: Inefficient O₂ utilization in renal cortex following chronic intermittent hypoxia

Corresponding author:

Julie O'Neill, PhD

Department of Physiology

School of Medicine

College of Medicine and Health

University College Cork

Cork, Ireland

Telephone: +353214905486

Abstract:

Chronic kidney disease (CKD) occurs in more than 50% of patients with obstructive sleep apnea (OSA). However, the impact of intermittent hypoxia (IH) on renal function and oxygen homeostasis is unclear. Male Sprague Dawley rats were exposed to IH (270 secs at 21% O₂; 90 secs hypoxia, 6.5% O₂ at nadir) for 4 h (AIH) or to chronic IH (CIH) for 8h/day for 2 weeks. Animals were anesthetized and surgically prepared for the measurement of mean arterial pressure (MAP), and left renal excretory function, renal blood flow (RBF), and renal oxygen tension (PO₂). AIH had no effect on MAP (123±14 versus (v) 129±14mmHg, mean±SEM, sham v IH). The CIH group were hypertensive (122±9 v 144±15mmHg, P<0.05). Glomerular filtration rate (GFR) (0.92±0.27 v 1.33±0.33ml/min), RBF (3.8±1.5 v 7.2±2.4ml/min) and transported sodium (TNa) (132±39 v 201±47μmol/min) were increased in the AIH group (all P<0.05). In the CIH group, GFR (1.25±0.28 v 0.86±0.28ml/min, P<0.05) and TNa (160±39 v 120±40μmol/min, P<0.05) were decreased, while RBF (4.13±1.5 v 3.08±1.5ml/min) was not significantly different. Oxygen consumption (QO₂) was increased in the AIH group (6.76±2.60 v 13.60±7.77μmol/min, P<0.05), but was not significantly altered in the CIH group (3.97±2.63 v 6.82±3.29μmol/min). Cortical PO₂ was not significantly different in the AIH group (46±4 v 46±3mmHg), but was decreased in the CIH group (44±5mmHg v 38±2mmHg, P<0.05). AIH: Renal oxygen homeostasis was preserved through a maintained balance between O₂ supply (RBF) and consumption (GFR). CIH: Mismatched TNa and QO₂ reflects inefficient O₂ utilization and thereby sustained decrease in cortical PO₂.

64 **Introduction:**

65 Chronic Kidney Disease (CKD) is characterized by structural and functional alterations in
66 glomeruli and renal tubules, which grossly impair filtration of blood plasma and the renal
67 handling of important electrolytes such as sodium. Classical clinical manifestations of CKD are
68 abnormal glomerular filtration and proteinuria (2). Indeed, it is well established that CKD is a
69 co-morbidity of disease pathologies such as diabetes mellitus, hypertension, chronic
70 glomerulonephritis and cystic kidney disease (14). A sustained decrease in renal tissue oxygen
71 availability has been reported in a variety of CKD models (10, 14, 27, 34). Importantly, it has
72 been demonstrated that sustained renal tissue hypoxia precedes albuminuria in a mouse model of
73 type 1 diabetes (12). Furthermore, proteinuria and immune cell infiltration resulted from an
74 increase in renal oxygen consumption and kidney tissue hypoxia in an animal model not
75 confounded by hyperglycemia or oxidative stress (chronic di-nitrophenol administration) (41).
76 Together these data provide evidence that kidney tissue hypoxia *per se* plays a potentially
77 important role in the pathogenesis of CKD.

78

79 It is now apparent that obstructive sleep apnea (OSA), which is characterized by repetitive cycles
80 of upper airway obstruction and resultant intermittent hypoxemia throughout the sleep cycle,
81 occurs in more than 50% of patients with CKD (2, 13). Moreover, clinical data suggest that
82 there is a correlation between OSA and glomerular hyperfiltration and proteinuria (2). Indeed a
83 number of possible pathophysiological links between OSA and CKD have been proposed and it
84 is plausible that exposure to CIH and thereby intermittent hypoxemia as well as sleep
85 fragmentation, which manifest in OSA, may contribute to CKD progression via the activation of
86 pro-oxidant (i.e. oxidative stress) (37,60), pro-inflammatory (NF-KB pathway) (43,59) and pro-
87 fibrotic pathways (sympathetic nervous system (SNS) and renin-aldosterone-angiotensin system

(RAAS) activation) (6,11,37). Indeed, the chronic repetitive cycles of blood deoxygenation/reoxygenation observed in experimental models of CIH have been shown to promote oxidative stress and inflammation both systemically and in the kidney (48,58)

However, the impact of IH *per se* on renal function is unclear and data describing the effects of IH on renal hemodynamics and tubular function, both of which are defective in CKD appears to be lacking. Moreover, given that a sustained decrease in kidney tissue PO₂ is now widely regarded as an important factor in the pathogenesis of secondary CKD (10, 14, 27) it would seem pertinent to determine both the immediate and long-term impact of IH on renal function and renal oxygen homeostasis. Thus the aim of the present study was twofold: Firstly, we aimed to determine the impact of acute IH (AIH) and CIH on renal hemodynamics, excretory function and metabolism. Secondly, we aimed to determine whether CIH-induced alterations in renal hemodynamics, excretory function and oxygen homeostasis are consistent with the current understanding of the pathogenesis of CKD.

Materials and Methods:

Ethical Approval

Male Sprague Dawley rats (8-10 weeks old) were obtained from the Biological Services Unit in University College Cork and maintained there under a 12h light-12h dark regimen at $20\pm 3^{\circ}\text{C}$. Animals received free access to standard chow and water. All experimental procedures were performed under the European Community Directive 86/609/EC and were approved by the local Animal Experimentation Ethics Committee (AEEC number: 2013/005). NIH guidelines for the care of experimental animals were adhered to throughout each protocol.

Animal Models of Intermittent Hypoxia (IH)

IH Profile

Animals were exposed to 10 cycles of IH per hour with each 6 min cycle consisting of 270 secs at 21% O_2 (normoxia) and 90secs of hypoxia with a gradual decline in chamber oxygen to a nadir of 6.5% O_2 .

Acute Intermittent Hypoxia (AIH)

Acute exposure of animals ($n=7$) to the above-described IH profile was carried out over a period of 4 hours (08:00/09:00 to 12:00/13:00 hrs) in a commercial plethysmography chamber. A dynamic O_2/N_2 controller (GSM-3 Gas Mixer, CWE Inc., USA) was used to create the IH profile and to deliver alternating levels of gas to a mixing chamber, which subsequently delivered gases to the plethysmography chamber. Chamber O_2 and CO_2 levels were monitored throughout the exposure.

Bedding was added to the chamber to enrich the environment and promote acclimation. Animals had *ad libitum* access to standard chow and water throughout the exposure. Once animals were placed in the chamber, a settling period of 30-40 minutes was sufficient to allow for the stabilization of respiration and environmental acclimation. The corresponding sham group ($n=6$) was exposed to air (21% O_2) under identical experimental conditions.

140 *Chronic Intermittent Hypoxia (CIH)*

141 Chronic exposure of animals (n=7) to IH was carried out over a period of 8 hours/day (08:00
142 to 16:00 hrs) for 2 weeks using a dynamic O₂/CO₂ controller (OxycyclerTM; Biospheric, NY,
143 USA). Chamber oxygen levels were measured continuously and controlled. Gas flow rates were
144 sufficient to prevent the accumulation of carbon dioxide in the chamber. Animals were placed in
145 their cage environment into environmental chambers, with *ad libitum* access to standard chow
146 and water. Sham animals (n=9) were housed in a similar environment with normoxia maintained
147 over 14 days. IH profiles for acute and chronic studies were matched. The IH profile was
148 designed so that the rate of de-oxygenation and re-oxygenation in all cycles were approximately
149 equivalent in each experimental context. Experiments were conducted in AIH exposed animals
150 and corresponding sham animals immediately following the 4hr exposure to IH to evaluate the
151 immediate and acute effects of repetitive de-oxygenation/re-oxygenation cycles. Experiments
152 were conducted in CIH exposed animals one day following the last IH exposure (ie day 15) to
153 evaluate the chronic and latent effects of repetitive de-oxygenation/re-oxygenation cycles.

154 *Surgical Protocol*

155 Following AIH or CIH exposure, animals were anesthetized via an intraperitoneal injection of
156 sodium pentobarbitone (Euthatal), (60 mg/kg) and placed on a heated pad so that body
157 temperature was maintained at 37°C. Adequacy of anesthesia was confirmed by absence of pedal
158 withdrawal to noxious pinch. Supplemental doses of anesthetic were administered if required. A
159 tracheostomy was performed (PP240 tubing) to facilitate respiration by spontaneous breathing. A
160 cannula was inserted into the right carotid artery (PP50) to facilitate the measurement of mean
161 arterial pressure (MAP) and into the right femoral vein to facilitate the infusion of Fluorescein
162 isothiocyanate-Inulin (FITC-Inulin) (Sigma Aldrich, St Louis, Missouri, USA) (10mg/kg/hr).

The animals were studied with their dorsal aspect exposed and the left kidney was exposed by a left subcostal flank incision. The left kidney was then stabilized in a cup and surrounded and covered by cotton wool soaked in paraffin oil (Sigma Aldrich, St Louis, Missouri, USA). This was carried out to ensure that the kidney remained moist at body temperature. The left renal vein was dissected and prepared for the withdrawal of blood samples for the measurement of blood gases and oxygen consumption (QO_2). 0.1 ml of venous blood was withdrawn very slowly from the renal vein using a 1 ml heparinized syringe and needle (27G) (BD Microlance). The entry site on the vein was sealed afterwards using an absorbable hemostatic gelatin sponge (Spongostan, Søberg, Denmark). The left renal artery was carefully dissected to facilitate the placement of a transit time ultrasound flow probe around the renal artery (renal blood flow (RBF) measurement) (Transconic. Systems, Ithaca, NY, USA). A cannula was inserted into the left ureter to facilitate the measurement of left renal function. Animals were allowed to stabilize for 45 minutes prior to the start of the experimental protocol. At the end of the experiment, animals were euthanized by an anesthetic overdose.

Experimental Protocol

The experimental protocol is summarized and described in Fig. 1.

Measurement of hemodynamic parameters

MAP was measured via the right carotid artery cannula, which was connected to a blood pressure transducer and a signal transduction amplifier. MAP was continuously monitored and recorded (AD Instruments, Hastings, UK). RBF was determined using a transonic flow probe, which was cupped around the renal artery and connected to a flow meter (Transonic Systems Inc, NY, USA). RBF was continuously monitored and recorded. Glomerular filtration rate (GFR) was determined by the clearance of FITC-Inulin. FITC fluorescence was measured in both urine and

plasma using a microplate reader (Wallac victor² 1420 multilabel counter, Perkin Elmer, USA). Blood gases and electrolytes were measured in blood withdrawn from the carotid artery and renal vein using the iSTAT system (Abbott Laboratories, Abbott Park, IL, USA).

Measurement of excretory parameters

Urine flow was determined gravimetrically at baseline. Urinary sodium concentrations were determined using flame spectrophotometry (model: M410, Sherwood Scientific, Ltd., UK). Urinary protein excretion (UPE) was measured using a BCA protein assay (Bio-Rad Laboratories, Hercules, California, USA). Urinary kidney injury molecule-1 (KIM-1) excretion was measured in sham (n=5) and CIH (n=5) groups using a KIM-1 ELISA kit (rat) purchased from GenWay Biotech, Inc. San Diego, California, USA. A multilabel plate reader was used at an absorbance of 450nm to quantify urinary protein concentrations and KIM-1 concentrations, after which both were normalized to urine flow rate.

In vivo measurement of oxygen tension in the renal cortex and medulla

At the end of each 40 min clearance period, PO₂ sensing probes (Product no: PO2 E series ref BF/OT/E) (fluorescence quenching oximetry) (OxyLite 2000, Oxford Optronics Ltd, Abingdon, UK) were used to measure both cortical and medullary PO₂. Probes were placed in micromanipulators. A small portion of the renal capsule was removed from the surface of the outer third of the kidney along the greater curvature. Once it was established that the tip of the probe was interfacing with the surface of the kidney (coincident with the partial pressure of oxygen falling from 120 mmHg to 100 mmHg), it was advanced 0.5-1.0 mm into the renal cortex. As soon as the recording became stable, a measurement was taken. The probe was then advanced a further 2.5 -3 mm in to the medulla (total depth 3.5-4 mm from kidney surface). Again once the recording became stable a measurement was taken. This was carried out several

times and the average cortical and medullary values were obtained. Importantly, after each set of cortical and medullary recordings the probe was completely removed from the kidney and reinserted in an area immediately adjacent (“undamaged area”) to the previous point of insertion.

Tissue Homogenization

Cortical and medullary tissue were weighed and homogenized in radio-immunoprecipitation assay RIPA lysis buffer (10% w/v) consisting of: 10x RIPA, deionized H₂O, sodium fluoride (NaF) (200mM) phenylmethylsulfonylfluoride (PMSF) (100mM), protease cocktail inhibitor ((5mM EDTA, 1 mM EGTA, 5µg/ml leupeptin, 5µg/ml aprotinin, 2µg/ml pepstatin, 120µg/ml Pefabloc, 2mM 1,10-phenanthroline and sodium orthovanadate (Naortho) (200mM) (All from Sigma Aldrich, Arklow, Wicklow, Ireland). Samples were homogenized on ice for 3 X 10 second bursts with 30 seconds lapsing between each burst. The homogenates were left on ice for 20 minutes with intermittent vortexing to allow cells to lyse. Samples were centrifuged at 15,366g at 4°C for 15 min to pellet debris from homogenates.

Nitric oxide (NO) and Oxidative Stress:

Urinary, plasma and renal tissue nitrate/nitrite (NO_x) levels were measured using a nitrate/nitrite colorimetric assay kit (Cayman Chemical, Michigan, USA) and all samples were assayed in duplicate. A multilabelled plate reader at an absorbance of 540nm quantified concentrations. Plasma and renal tissue thiobarbituric acid reactive substances (TBARS) were measured using a laboratory based thiobarbituric acid assay (Persson et al 2014) and the concentration of TBARS in the kidney and plasma was quantified by a multilabelled fluorescent plate reader (excitation: 523nm, emission: 553nm).

Markers of renal inflammation

Renal cortical tissue homogenates were profiled for the following cytokine levels: Interferon (IFN)- γ , Interleukin-1 β (IL-1 β), IL-4, IL-5, IL-6, keratinocyte chemoattractant/growth related oncogene (KC/GRO), IL-10, IL-13 and tumor necrosis factor (TNF)- α . This was carried out by sandwich immunoassay methods using commercially available detection kits (V-plex Pro-inflammatory Panel 2 (rat) kit; Meso Scale Discovery, Rockville, Maryland, USA) as per manufacturer's instruction. 200 μ g of protein from each tissue sample was loaded in duplicate into wells. Plates were analyzed using a QuickPlex SQ 120 plate reader (Meso Scale Discovery, Rockville, Maryland, USA.) IL-4, IL-5 and IL-13 levels could not be established in the renal cortex in the present study because their levels were below the limits of detection. INF- γ was not detected in 1 AIH and 1 sham sample.

Gene Expression

RNA extraction and gene reverse transcription

RNA extraction and reverse transcription was carried out as previously described (29). Briefly, RNA was extracted, using Tripure Isolation Reagent (Roche Diagnostics Ltd., West Sussex, UK), from frozen kidney tissue (25-50mg per sample) using a standard laboratory homogeniser (Omni-Inc., Kennesaw, Georgia, USA) as per the manufacturer's instructions, with an additional chloroform wash step during phase separation. Following isolation, RNA was treated with TURBO DNA-free Kit (Life Technologies, Bio-Sciences, Dun Laoghaire, Ireland). RNA quantity and purity was assessed by spectrophotometry with a Nanodrop 1000 (Thermo Scientific, Wilmington, Delaware, USA). RNA integrity was assessed using an agarose gel electrophoresis system (E-gel, Life Technologies, Carlsbad, California, USA) and visualization of clear 18S and 28S ribosomal RNA bands. RNA was reverse transcribed using Transcriptor First Strand cDNA Synthesis Kit (Roche Diagnostics Ltd.) as per the manufacturer's

instructions.

qPCR

cDNA was amplified using Realtime ready Catalog or Custom Assays (Roche Diagnostics Ltd. Basal, Switzerland) and Fast Start Essential DNA Probe Master (Roche Diagnostics Ltd. Basal, Switzerland) as per the manufacturer's instructions, using the LightCycler 96 (Roche Diagnostics Ltd. Basal, Switzerland) on 96-well plates. All reactions were performed in duplicate. Data were normalized to a reference gene, *hprt1*. Relative expression of HIF-1 α , NF- κ B, NOS-1, NOS-3, VEGF, NOX-4 and HO-1 (Roche Diagnostics Ltd. Basal, Switzerland) was calculated using the $\Delta\Delta$ CT method to normalize expression to the reference gene with changes in expression displayed as a fold change over the control group. Three sham kidney tissue samples corresponding with the AIH group were depleted and thus mRNA levels could not be measured for these animals. Therefore, sham samples corresponding to AIH and CIH studies were pooled for the purpose of data analysis (sham n=8-10, AIH, n=6 and CIH, n=7). An outlier was removed from the sham group in the analysis of HO-1 levels.

Calculations

GFR was calculated using: $GFR = U \cdot UV / P$, where U = urinary [FITC inulin], UV = urine volume, P = plasma [FITC inulin]. Renal vascular resistance (RVR) was determined by: $RVR = (MAP/RBF)$. *In vivo* renal oxygen consumption (QO_2) was estimated from the arteriovenous difference in oxygen content and was given by: $QO_2 = \text{arterio-venous difference in oxygen content} \cdot RBF$, where blood oxygen content = $1.34 \cdot \text{Hemoglobin oxygen saturation} \cdot \text{Hemoglobin concentration} + \text{blood } PO_2 \cdot 0.003$. Tubular sodium transport (TNa) was calculated by: $TNa = [PNa] \cdot GFR - [UNa] \cdot UV$, where [PNa] = plasma sodium concentration and [UNa] = urinary

sodium concentration. Fractional sodium excretion = sodium clearance/GFR, where sodium clearance= $[UNa] \cdot UV/[PNa]$.

Statistical analysis

Data are presented as mean \pm SEM. All statistical analyses were performed using GraphPad Prism (GraphPad Software, San Diego, CA, USA). All data were analyzed using 2x2 ANOVA with a Bonferroni post-hoc test unless otherwise specified. There were 2 multiple comparisons made per family. Differences were deemed to be statistically significant when $P < 0.05$. The critical value of P in this context was two sided. Ordinary least products regression analysis (Deming model II) was used to calculate lines of best fit for TNa and QO_2 . Renal mRNA expression levels of NF- κ B, HIF-1 α , NOS-1, NOS-3, NOX4, HO-1 and VEGF were analyzed using a one way ANOVA. Urinary KIM-1 levels in sham versus CIH animals were compared using an unpaired t-test.

Results:

General

Exposure of animals to either AIH or CIH had no significant effect on body weight (Table 1). The partial pressure of oxygen in arterial blood (PaO_2) was higher and the partial pressure of carbon dioxide in arterial blood ($PaCO_2$) was lower in animals exposed to CIH compared with

sham control group (Table 1), revealing a mild persistent hyperventilation with metabolic compensation, indicative of long-term facilitation (LTF) of breathing (22), which can persist under normoxic conditions for as long as 3 days following exposure to CIH (22,23). Hematocrit and hemoglobin levels in arterial blood were significantly elevated in animals exposed to CIH compared with the corresponding sham control group (Table 1).

Hemodynamic parameters

Exposure to AIH had no significant effect on MAP, whereas animals exposed to CIH were hypertensive compared with the corresponding controls (Fig 2A). Exposure of animals to AIH resulted in an increase in GFR and RBF (both $P < 0.05$), whereas exposure of animals to CIH had the opposite effect (Interaction: Gas x Duration: $P = 0.004$ and $P = 0.005$, respectively) (Fig 2B and C). Correspondingly, RVR was lower in the animals exposed to AIH and higher in the animals exposed to CIH (Interaction: Gas x Duration: $P = 0.004$) (Fig 2D).

Excretory parameters (Table 2)

UF, UNaV, FENa and sodium clearance were not significantly altered by either AIH or CIH exposures. However, the results of the 2-way ANOVA performed on the UF data revealed a significant interaction, with opposing effects on this variable in the context of acute versus chronic exposures (Table 2). Urinary protein excretion (UPE) was not significantly different between animals exposed to AIH and the corresponding sham control group. Conversely, a modest proteinuria was evident in animals exposed to CIH ($P = 0.09$) (Table 2).

Sodium Transport and Renal Oxygen Consumption

Sodium transport (TNa) was greater in animals exposed to AIH, whereas TNa was reduced in animals exposed to CIH (Interaction: Gas x Duration: $P = 0.002$) (Fig 3A). Renal oxygen

consumption (QO_2) was also greater in animals exposed to AIH (Fig 3B). Conversely, exposure of animals to CIH had no significant impact on QO_2 (Fig 3B). The relationship between TNa and QO_2 was also examined using regression analysis in groups exposed to either AIH or CIH. The slope of the relationship between TNa and QO_2 was compared (Fig 3C and D). Neither AIH nor CIH significantly affected the slope of the relationship between TNa and QO_2 (Fig 3C and D). We interpret this to mean that sham and IH animals exhibit the same increase in renal QO_2 per unit change TNa (no difference in the efficiency of TNa). However, the elevation of the relationship between TNa and QO_2 was significantly greater in animals exposed to CIH ($P=0.001$). Thus, at any given TNa, CIH animals exhibit a significantly higher renal QO_2 .

Renal Oxygen Tension

Exposure of animals to AIH had no significant effect on tissue oxygen availability in either the renal cortex or medulla (Fig 4A and B). Conversely, exposure to CIH was associated with significantly lower PO_2 in the renal cortex compared with corresponding sham controls. There was no significant difference in medullary PO_2 values between CIH and sham groups (Fig 4A and B).

Nitric Oxide

NO was measured in the plasma, urine and in the renal cortex and medulla in all groups (Table 3). Urinary NO_x excretion was similar in all groups. NO_x concentration in the plasma and renal cortex was significantly lower both in AIH and CIH groups compared with corresponding sham control groups.

Oxidative Stress

TBARS concentration was measured in the plasma and in the renal cortex and medulla (Table 3) in all groups. Enhanced lipid peroxidation was not evident in animals exposed to either AIH or CIH in plasma, renal cortex or renal medulla.

Inflammatory Profile: Renal Cortex

IFN- γ levels were significantly increased in animals exposed to AIH (Table 4). The concentrations of the other detectable inflammatory cytokines in renal cortex did not significantly differ between groups (Table 4).

Gene expression: Whole kidney

Renal *NF- κ B*, *HIF-1 α* , *HO-1*, *VEGF*, *NOS-1*, *NOS-3* and *NOX-4* gene expression did not significantly differ between sham, AIH and CIH groups (Table 5).

Discussion:

The present study sought to determine the impact of IH exposure on renal function and oxygen homeostasis with a view to a better understanding of the potential role this stimulus might play in the pathogenesis of CKD. To this end, animals were exposed to a moderate IH profile (similar to what might be observed in patients with OSA) either acutely for four hours or chronically for eight hours per day for two weeks prior to the *in vivo* measurement of renal hemodynamics,

excretory function and oxygen homeostasis. The first finding of the present study was that renal tissue oxygen availability (PO_2) was preserved in animals exposed to AIH due to reciprocal increases in renal QO_2 , and O_2 delivery via RBF. The second finding was that significant decreases in tissue oxygen was evident in the renal cortex of animals exposed to CIH, which most likely resulted from elevations in transport unrelated oxygen consumption (basal metabolism). Importantly, the altered NO bioavailability and sustained decrease in tissue PO_2 in the renal cortex of animals exposed to CIH is consistent with previous observations in other animal models of CKD, such as diabetes and hypertension (28, 30, 33, 34, 38, 40, 55).

In the present study, both RBF and GFR were higher and RVR was lower in animals exposed to IH for four hours. Viewed collectively, these data provide evidence for an acute hyperemia and afferent arteriolar dilation (7,45). Analysis of the kidney tissue was carried out in an effort to determine possible mechanisms underlying IH-induced hyperemia. The potential role played by NO in mediating this response is not entirely clear at present. Indeed plasma and renal tissue levels of NOx metabolites reveal that a four hour IH exposure decreased NO production. This observation is consistent with the findings of others in mouse aorta (52), but is not consistent with the observed hyperemia in the present study. Indeed, exposure to AIH had no significant impact upon NOS-1 or NOS-3 mRNA expression levels, indicating that endothelial and neuronal nitric oxide synthase were unaffected at a transcriptional level. However, the present observations are limited because we did not measure for NOS-1 and NOS-3 activity levels, which could potentially be altered thereby accounting for the decrease in NOx metabolites observed in the present study. It is also important to acknowledge that the regulation of NO bioavailability/activity is complex and not just solely dependent upon NOS-mediated NO production *per se*. It can also be influenced by other factors such as arginase activity, L-citrulline concentration, superoxide anion production and the availability of NO associated signaling

molecules such as soluble guanylate cyclase (sGC) and cyclic guanosine monophosphate (cGMP) (39, 57). Thus, NO cannot be ruled out as a potential mediator of the hyperemia observed in the AIH group.

Kidney tissue was also investigated for evidence of Hemeoxygenase-1 (HO-1) upregulation at the transcriptional level because HO-1 synthesizes carbon monoxide (CO) a potent vasodilator. Previous studies have demonstrated that acute IH exposure and ischemia reperfusion injury are both coincident with HO-1 upregulation in the liver, brain and kidney tissue (21, 44, 50). AIH exposure had no significant effect on HO-1 expression and thus there is no evidence that CO was mediating the renal hyperemia observed in the present study. Of interest, the cytokine profile analysis of renal cortical tissue demonstrated that IFN- γ levels were significantly increased following AIH exposure. IFN- γ is an inflammatory cytokine that is known to acutely dilate resistance arteries in uterine tissue (5, 16). Indeed, the literature suggests that an acute elevation in IFN- γ , stimulates inducible NOS (iNOS) in endothelial cells, which can in turn increase local NO production (26). We did not measure iNOS expression or activity and thus the potential role of the IFN- γ /iNOS/NO pathway in mediating renal hyperemia in response to an acute exposure to IH should be addressed in subsequent studies.

AIH-induced alterations in hemodynamic parameters were paralleled by reciprocal alterations in metabolism, as evidenced by heightened TNa and QO_2 . Consistent with the observations of others in several animal models, increased TNa and QO_2 observed in the present study is most likely related to increases in GFR (9, 15, 30, 35). Indeed, it is now well established that pathological or pharmacological elevations in GFR result in corresponding increases in the filtered load of sodium, which in turn increase the reabsorptive work of the kidney, particularly in the proximal tubules (9, 15, 30) The increased TNa observed in this study following AIH

exposure reflects a rise in the activity of tubular sodium transporters whose function is either primarily or secondarily dependent upon the hydrolysis of ATP. The linear relationship between TNa and QO_2 was not altered by AIH exposure, indicating that the raised QO_2 was solely related to a reciprocal rise in TNa of equal magnitude, and was not due to reductions in the efficiency of TNa (9,10). Overall these data suggest that the elevated QO_2 observed in AIH rats resulted from an increase in the transport related demand for ATP. Importantly, under these experimental conditions renal tissue oxygen availability in the cortex and medulla was maintained within normal limits because the balance was preserved between oxygen supply and demand.

In agreement with previous reports, animals exposed to CIH were hypertensive (17, 20, 49). Of interest, in the present study, CIH exposure had opposing effects on renal hemodynamics compared with AIH, such that animals presented with a relatively lower RBF and GFR, and a higher RVR. The hemodynamic changes in response to CIH were accompanied by a modest proteinuria, which is manifest in a proportion patients with OSA (8, 24), and consistent with CIH induced structural changes in the glomeruli in an animal model (1). Also of note was a 43% increase in urinary KIM-1 excretion rate in animals exposed to CIH, which is indicative of proximal tubular injury at the very early stages of CKD (18). Importantly, the above hemodynamic responses observed in this study are consistent with the reported impact of IH on vascular reactivity in other tissues. CIH exposure has been shown to increase the vasoconstrictor response to endothelin and norepinephrine in rat mesenteric arteries (3) and in the vascular bed of the rat cremaster muscle (51), indicating that CIH primes the blood vessels for constriction. Importantly, Tahawi et al 2001 also observed weakened vasoconstrictor responses to the NOS inhibitor L-NAME, indirectly indicating that these blood vessels have impaired vasodilation due to reductions in the production of NO (51). In the present study, CIH-induced reductions in GFR and RBF were associated with a decrease in NO metabolites both systemically and in renal

tissue, indicating that vasoconstriction was associated with a concomitant reduction in the production of NO. These observations are in agreement with the current literature where it is well established that reduced NO production impairs renal blood perfusion (13).

On the other hand, there was no association between the reductions in RBF and GFR observed in CIH-exposed animals and oxidative stress (as measured by lipid peroxidation), with equivalent levels both in the plasma and kidney tissue of all groups. These data were surprising given that reactive oxygen species (ROS) are known vasoconstrictors and have been reported to accumulate both systemically and in the kidney in mouse and rat models of CIH (19, 37, 48). However, in the latter studies, ROS accumulation was only evident after more than 6-8 weeks of exposure, substantially longer than the 2 week exposure to IH used in the present study. These studies also demonstrated that antioxidant enzymes such as superoxide dismutase (SOD) were upregulated after 3 days of IH exposure. Of interest, SOD is downregulated after 8 weeks of exposure to IH, which coincided with the renal accumulation of ROS (48). In the context of the present study, it may well be that there was an upregulation in the expression and activity of antioxidant enzymes accounting for the absence of ROS accumulation in the plasma and kidney of rats exposed to CIH, and perhaps AIH.

The metabolic consequences of the diminished GFR observed in animals exposed to CIH were reflected in corresponding reductions in TNa, but not in QO₂. The regression analysis performed on this data set indicates that the nature of the relationship between the two variables was altered in the CIH group, such that global renal QO₂ was significantly greater at any given level of TNa. These observations suggest that sodium transport efficiency was reduced in the CIH group. Indeed, one might be tempted to assume that a decrease in GFR and thereby the proximal reabsorption of sodium could potentially lead to a compensatory shift in TNa to more distal

nephron segments where the metabolic cost of sodium reabsorption is higher, i.e. the medullary thick ascending limb (mTAL) (9, 14, 30). However, in the context of the present study this is unlikely because MPO_2 was not significantly decreased in conjunction with GFR and TNa.

Alternatively these data could reflect an increase in transport unrelated QO_2 /basal metabolism, which could also potentially explain why QO_2 was not decreased in conjunction with TNa and GFR in the group exposed to CIH. Renal NO metabolites were also reduced significantly in the renal cortex of animals exposed to CIH indicating a possible reduction in the biosynthesis of NO. Thus one plausible cause for the observed discrepancy between GFR/TNa and QO_2 in the present study is that a reduction in NO bioavailability diminished the tonic inhibitory effect of NO on mitochondrial respiration, thereby increasing basal mitochondrial QO_2 (15, 25, 57). Whether, the mismatch between TNa and QO_2 resulted from an increase in transport related QO_2 or basal metabolism is unclear. Either way, the net effect was a reduction in tissue PO_2 in the renal cortex in animals exposed to CIH. Importantly, these observations are consistent with previous observations of others in various animal models of kidney disease (28, 30, 33, 34, 55).

It has been reported that chronic sustained decreases in oxygen availability in the kidney activate pro-inflammatory pathways (Ohtomo et al 2008, Nordquist et al 2015). Moreover, experimental data suggests that renal HIF-1 α activation contributes to the activation of pro-inflammatory pathways in animal models of diabetes (28, 31). In the present study, CIH-induced reduction in cortical tissue oxygen tension was not associated with HIF-1 α or NF- κ B activation at the transcriptional level, although there was a trend for elevated levels in the CIH-exposed kidney. Moreover, exposure to CIH did not significantly affect the transcriptional expression of other HIF response genes such as NOS-1, NOS-3, VEGF or HO-1. On the contrary, blood gas analysis revealed that hemoglobin and hematocrit were both significantly elevated in CIH-exposed

animals, providing some indirect evidence of renal HIF-1 α induced up-regulation of erythropoietin, a HIF response gene (42, 47), perhaps transiently, over the course of the 2 week exposure to IH. Others have demonstrated IH-induced renal tissue HIF-1 α upregulation from weeks 6-9 following the onset of IH exposure (19). In agreement with the present observations, Sun et al. 2015 demonstrated that HIF-1 α protein expression was not significantly upregulated in mice exposed to IH for 2 weeks (48), suggesting that HIF-1 α maybe transiently activated during 2 weeks of IH exposure, whereas longer duration exposures may result in a more sustained period of HIF-1 α activation.

Finally, the present study provides no evidence for a pronounced renal inflammatory response after 2 weeks of IH exposure either at the gene or protein level, with IFN- γ the only inflammatory cytokine that was found to be increased in the renal cortex following exposure to IH. Of note, Lu et al 2017 observed increases in TNF- α and IL-6 only after 6 weeks of IH exposure in rats and Sun et al 2015 demonstrated that inflammatory markers such as cell adhesion molecules (ICAM1) and plasminogen activator inhibitor (PAI) were equivalent to control levels following a 2 week exposure to IH in mice (19, 48). Our data suggest that a 2 week exposure to IH and the resultant decrease in cortical tissue oxygen tension at this early stage were not associated with a robust inflammatory response in the renal cortex. We speculate that IH exposures of longer duration potentially result in decreases in renal oxygen tension of greater magnitude, which in turn could stimulate a more robust inflammatory response.

Limitations:

It is not clear whether the reduction in renal cortex oxygen tension observed in animals exposed to CIH was related to intermittent hypoxia *per se* or whether it is a consequence of hypertension. It is established that kidney tissue hypoxia is present in animal models of hypertension such as

the spontaneously hypertensive rat (SHR) (54, 56). Impaired renal blood flow may in part contribute to kidney tissue hypoxia in the SHR, but reductions in the efficiency of oxygen utilization for sodium transport have also been reported to play a major role (54). Thus it may well be that the dysregulated oxygen homeostasis observed in the present study is an indirect consequence of IH-induced hypertension as opposed to renal tissue IH *per se*. It would be interesting to explore the temporal changes in renal tissue oxygen tension in the transition from short-term to long-term IH exposure and the development of hypertension. Renal tissue hypoxia and consequential aberrant afferent signaling from the kidneys to the brainstem may be a critical component of the development and/or maintenance of high blood pressure (36). Another limitation of the present study is that we did not measure tissue levels of superoxide or antioxidant enzymes. Thus the putative role of altered redox signaling in the kidney in response to IH exposure remains unclear.

Conclusions:

The metabolic consequences of increased GFR in animals exposed to AIH are reflected by corresponding increases in TNa and QO_2 . Renal PO_2 was not altered in conjunction with QO_2 indicating that AIH exposure activates a compensatory mechanism in the kidney whereby O_2 delivery (RBF) and consumption, although elevated remain balanced, thereby preserving tissue O_2 availability. The metabolic consequences of a diminished GFR in animals exposed to CIH were reflected by reductions in TNa, but not in QO_2 . The mismatch between TNa and QO_2 reflects a decrease in the metabolic efficiency of sodium transport. Consequently, a decrease in tissue PO_2 in the renal cortex was evident after 2 weeks of CIH exposure. These perturbations in renal function and oxygen homeostasis were associated with corresponding reductions in the systemic and renal production of NO metabolites. It is clear that 2 weeks of CIH exposure induces changes in renal function and oxygen homeostasis that are consistent with aspects of the

current understanding of CKD. However, the precise mechanisms by which cortical tissue hypoxia might contribute to CKD in this model require further investigation. Moreover, future studies are needed to determine the impact of IH exposure on kidney oxygen homeostasis preceding the development of the CIH-induced hypertensive phenotype.

Acknowledgements

We are grateful to Mr. Kieran McDonnell for technical support. Funded by the Department of Physiology, University College Cork, Ireland. We are also grateful to the Palm Laboratory at the Uppsala University for the TBARS protocol.

Conflict of Interest

None to declare.

Author contributions

JON & KDOH conceived the idea of the study; JON, EFL, MAA & KDOH designed the study; JON performed *in vivo* experiments with the assistance of OB; JON, SD, OB & GJ performed assays and PCR; JON and OB analyzed data; JON drafted the manuscript with revisions from KDOH; all authors provided intellectual input; all authors approved the final manuscript.

577
578
579
580
581
582
583
584
585
586

References

- 587 1. Abuyassin, B., Sharma, K., Ayas, N. T. and Laher, I. (2015) 'Obstructive Sleep
588 Apnea and Kidney Disease: A Potential Bidirectional Relationship?', *J Clin*
589 *Sleep Med*, 11(8), pp. 915-24.
- 590 2. Adeseun, G. A. and Rosas, S. E. (2010) 'The impact of obstructive sleep apnea
591 on chronic kidney disease', *Curr Hypertens Rep*, 12(5), pp. 378-83.
- 592 3. Allahdadi, K. J., Walker, B. R. and Kanagy, N. L. (2005) 'Augmented
593 endothelin vasoconstriction in intermittent hypoxia-induced
594 hypertension', *Hypertension*, 45(4), pp. 705-9.
- 595 4. Asai, H., Hirata, J., Hirano, A., Hirai, K., Seki, S. and Watanabe-Akanuma, M.
596 (2016) 'Activation of aryl hydrocarbon receptor mediates suppression of
597 hypoxia-inducible factor-dependent erythropoietin expression by indoxyl
598 sulfate', *Am J Physiol Cell Physiol*, 310(2), pp. C142-50.
- 599 5. Ashkar, A. A. and Croy, B. A. (1999) 'Interferon-gamma contributes to the
600 normalcy of murine pregnancy', *Biol Reprod*, 61(2), pp. 493-502.
- 601 6. Calhoun, D. A., Nishizaka, M. K., Zaman, M. A. and Harding, S. M. (2004)
602 'Aldosterone excretion among subjects with resistant hypertension and
603 symptoms of sleep apnea', *Chest*, 125(1), pp. 112-7.
- 604 7. Carmines, P. K. (2010) 'The renal vascular response to diabetes', *Curr Opin*
605 *Nephrol Hypertens*, 19(1), pp. 85-90.
- 606 8. Casserly, L. F., Chow, N., Ali, S., Gottlieb, D. J., Epstein, L. J. and Kaufman, J.
607 S. (2001) 'Proteinuria in obstructive sleep apnea', *Kidney Int*, 60(4), pp. 1484-9.
- 608 9. Cohen, J. J. (1986) 'Relationship between energy requirements for Na⁺
609 reabsorption and other renal functions', *Kidney Int*, 29(1), pp. 32-40.

10. Evans, R. G., Harrop, G. K., Ngo, J. P., Ow, C. P. and O'Connor, P. M. (2014) 'Basal renal O₂ consumption and the efficiency of O₂ utilization for Na⁺ reabsorption', *Am J Physiol Renal Physiol*, 306(5), pp. F551-60.
11. Fletcher, E. C., Lesske, J., Behm, R., Miller, C. C., Stauss, H. and Unger, T. (1992) 'Carotid chemoreceptors, systemic blood pressure, and chronic episodic hypoxia mimicking sleep apnea', *J Appl Physiol* (1985), 72(5), pp. 1978-84.
12. Franzén, S., Pihl, L., Khan, N., Gustafsson, H. and Palm, F. (2016) 'Pronounced kidney hypoxia precedes albuminuria in type 1 diabetic mice', *Am J Physiol Renal Physiol*, 310(9), pp. F807-9.
13. Fu, Q., Colgan, S. P. and Shelley, C. S. (2016) 'Hypoxia: The Force that Drives Chronic Kidney Disease', *Clin Med Res*, 14(1), pp. 15-39.
14. Hansell, P., Welch, W. J., Blantz, R. C. and Palm, F. (2013) 'Determinants of kidney oxygen consumption and their relationship to tissue oxygen tension in diabetes and hypertension', *Clin Exp Pharmacol Physiol*, 40(2), pp. 123-37.
15. Laycock, S. K., Vogel, T., Forfia, P. R., Tuzman, J., Xu, X., Ochoa, M., Thompson, C. I., Nasjletti, A. and Hintze, T. H. (1998) 'Role of nitric oxide in the control of renal oxygen consumption and the regulation of chemical work in the kidney', *Circ Res*, 82(12), pp. 1263-71.
16. Leonard, S., Lima, P. D., Croy, B. A. and Murrant, C. L. (2013) 'Gestational modification of murine spiral arteries does not reduce their drug-induced vasoconstrictive responses in vivo', *Biol Reprod*, 89(6), pp. 139.
17. Lesske, J., Fletcher, E. C., Bao, G. and Unger, T. (1997) 'Hypertension caused by chronic intermittent hypoxia--influence of chemoreceptors and sympathetic nervous system', *J Hypertens*, 15(12 Pt 2), pp. 1593-603.
18. Liu, X., Guan, Y., Xu, S., Li, Q., Sun, Y., Han, R. and Jiang, C. (2016) 'Early Predictors of Acute Kidney Injury: A Narrative Review', *Kidney Blood Press Res*, 41(5), pp. 680-700.
19. Lu, W., Kang, J., Hu, K., Tang, S., Zhou, X., Yu, S. and Xu, L. (2017) 'Angiotensin-(1-7) relieved renal injury induced by chronic intermittent hypoxia in rats by reducing inflammation, oxidative stress and fibrosis', *Braz J Med Biol Res*, 50(1), pp. e5594.
20. Lucking, E. F., O'Halloran, K. D. and Jones, J. F. (2014) 'Increased cardiac output contributes to the development of chronic intermittent hypoxia-induced hypertension', *Exp Physiol*, 99(10), pp. 1312-24.
21. Maeda, H. and Yoshida, K. (2016) 'Intermittent hypoxia upregulates hepatic heme oxygenase-1 and ferritin-1, thereby limiting hepatic pathogenesis in rats fed a high-fat diet', *Free Radic Res*, 50(7), pp. 720-31.
22. Mateika, J. H. and Narwani, G. (2009) 'Intermittent hypoxia and respiratory plasticity in humans and other animals: does exposure to intermittent hypoxia promote or mitigate sleep apnoea?', *Exp Physiol*, 94(3), pp. 279-96.
23. McGuire, M., Zhang, Y., White, D. P. and Ling, L. (2003) 'Chronic intermittent hypoxia enhances ventilatory long-term facilitation in awake rats', *J Appl Physiol* (1985), 95(4), pp. 1499-508.

24. Mello, P., Franger, M., Boujaoude, Z., Adaimy, M., Gelfand, E., Kass, J. and Weisberg, L. S. (2004) 'Night and day proteinuria in patients with sleep apnea', *Am J Kidney Dis*, 44(4), pp. 636-41.
25. Moncada, S. and Higgs, A. (1993) 'The L-arginine-nitric oxide pathway', *N Engl J Med*, 329(27), pp. 2002-12.
26. Morikawa, A., Koide, N., Kato, Y., Sugiyama, T., Chakravorty, D., Yoshida, T. and Yokochi, T. (2000) 'Augmentation of nitric oxide production by gamma interferon in a mouse vascular endothelial cell line and its modulation by tumor necrosis factor alpha and lipopolysaccharide', *Infect Immun*, 68(11), pp. 6209-14.
27. Nangaku, M. (2006) 'Chronic hypoxia and tubulointerstitial injury: a final common pathway to end-stage renal failure', *J Am Soc Nephrol*, 17(1), pp. 17-25.
28. Nordquist, L., Friederich-Persson, M., Fasching, A., Liss, P., Shoji, K., Nangaku, M., Hansell, P. and Palm, F. (2015) 'Activation of hypoxia-inducible factors prevents diabetic nephropathy', *J Am Soc Nephrol*, 26(2), pp. 328-38.
29. O'Leary, A. J. and O'Halloran, K. D. (2016) 'Diaphragm muscle weakness and increased UCP-3 gene expression following acute hypoxic stress in the mouse', *Respir Physiol Neurobiol*, 226, pp. 76-80.
30. O'Neill, J., Fasching, A., Pihl, L., Patinha, D., Franzén, S. and Palm, F. (2015) 'Acute SGLT inhibition normalizes O₂ tension in the renal cortex but causes hypoxia in the renal medulla in anaesthetized control and diabetic rats', *Am J Physiol Renal Physiol*, 309(3), pp. F227-34.
31. Ohtomo, S., Nangaku, M., Izuhara, Y., Takizawa, S., Strihou, C. and Miyata, T. (2008) 'Cobalt ameliorates renal injury in an obese, hypertensive type 2 diabetes rat model', *Nephrol Dial Transplant*, 23(4), pp. 1166-72.
32. Ow, C. P. C., Ngo, J. P., Ullah, M. M., Hilliard, L. M. and Evans, R. G. (2018) 'Renal hypoxia in kidney disease: Cause or consequence?', *Acta Physiol (Oxf)*, 222(4), pp. e12999.
33. Palm, F., Buerk, D. G., Carlsson, P. O., Hansell, P. and Liss, P. (2005) 'Reduced nitric oxide concentration in the renal cortex of streptozotocin-induced diabetic rats: effects on renal oxygenation and microcirculation', *Diabetes*, 54(11), pp. 3282-7.
34. Palm, F., Cederberg, J., Hansell, P., Liss, P. and Carlsson, P. O. (2003) 'Reactive oxygen species cause diabetes-induced decrease in renal oxygen tension', *Diabetologia*, 46(8), pp. 1153-60.
35. Patinha, D., Fasching, A., Pinho, D., Albino-Teixeira, A., Morato, M. and Palm, F. (2013) 'Angiotensin II contributes to glomerular hyperfiltration in diabetic rats independently of adenosine type I receptors', *Am J Physiol Renal Physiol*, 304(5), pp. F614-22.
36. Patinha, D., Pijacka, W., Paton, J. F. R. and Koeners, M. P. (2017) 'Cooperative Oxygen Sensing by the Kidney and Carotid Body in Blood Pressure Control', *Front Physiol*, 8, pp. 752.

37. Peng, Y. J., Overholt, J. L., Kline, D., Kumar, G. K. and Prabhakar, N. R. (2003) 'Induction of sensory long-term facilitation in the carotid body by intermittent hypoxia: implications for recurrent apneas', *Proc Natl Acad Sci U S A*, 100(17), pp. 10073-8.
38. Persson, M. F., Franzén, S., Catrina, S. B., Dallner, G., Hansell, P., Brismar, K. and Palm, F. (2012a) 'Coenzyme Q10 prevents GDP-sensitive mitochondrial uncoupling, glomerular hyperfiltration and proteinuria in kidneys from db/db mice as a model of type 2 diabetes', *Diabetologia*, 55(5), pp. 1535-43.
39. Persson, P., Fasching, A., Teerlink, T., Hansell, P. and Palm, F. (2014) 'L-Citrulline, but not L-arginine, prevents diabetes mellitus-induced glomerular hyperfiltration and proteinuria in rat', *Hypertension*, 64(2), pp. 323-9.
40. Persson, P., Hansell, P. and Palm, F. (2012b) 'NADPH oxidase inhibition reduces tubular sodium transport and improves kidney oxygenation in diabetes', *Am J Physiol Regul Integr Comp Physiol*, 302(12), pp. R1443-9.
41. Persson, M.F., Persson, P., Fasching, A., Hansell, P., Nordquist, L., Palm, F. (2013) 'Increased kidney metabolism as a pathway to kidney tissue hypoxia and damage: effects of triiodothyronine and dinitrophenol in normoglycemic rats', *Adv Exp Med Biol* 289:9-14
42. Prass, K., Scharff, A., Ruscher, K., Löwl, D., Muselmann, C., Victorov, I., Kapinya, K., Dirnagl, U. and Meisel, A. (2003) 'Hypoxia-induced stroke tolerance in the mouse is mediated by erythropoietin', *Stroke*, 34(8), pp. 1981-6.
43. Quercioli, A., Mach, F. and Montecucco, F. (2010) 'Inflammation accelerates atherosclerotic processes in obstructive sleep apnea syndrome (OSAS)', *Sleep Breath*, 14(3), pp. 261-9.
44. Regner, K. R. and Roman, R. J. (2012) 'Role of medullary blood flow in the pathogenesis of renal ischemia-reperfusion injury', *Curr Opin Nephrol Hypertens*, 21(1), pp. 33-8.
45. Ren, Y., Garvin, J. L. and Carretero, O. A. (2001) 'Efferent arteriole tubuloglomerular feedback in the renal nephron', *Kidney Int*, 59(1), pp. 222-9.
46. Ricksten, S. E., Bragadottir, G. and Redfors, B. (2013) 'Renal oxygenation in clinical acute kidney injury', *Crit Care*, 17(2), pp. 221.
47. Souvenir, R., Flores, J. J., Ostrowski, R. P., Manaenko, A., Duris, K. and Tang, J. (2014) 'Erythropoietin inhibits HIF-1 α expression via upregulation of PHD-2 transcription and translation in an in vitro model of hypoxia-ischemia', *Transl Stroke Res*, 5(1), pp. 118-27.
48. Sun, W., Yin, X., Wang, Y., Tan, Y., Cai, L., Wang, B., Cai, J. and Fu, Y. (2012) 'Intermittent hypoxia-induced renal antioxidants and oxidative damage in male mice: hormetic dose response', *Dose Response*, 11(3), pp. 385-400.
49. Sunderram, J. and Androulakis, I. P. (2012) 'Molecular mechanisms of chronic intermittent hypoxia and hypertension', *Crit Rev Biomed Eng*, 40(4), pp. 265-78.
50. Sunderram, J., Semmlow, J., Patel, P., Rao, H., Chun, G., Agarwala, P., Bhaumik, M., Le-Hoang, O., Lu, S. E. and Neubauer, J. A. (2016) 'Heme

- oxygenase-1-dependent central cardiorespiratory adaptations to chronic intermittent hypoxia in mice', *J Appl Physiol* (1985), 121(4), pp. 944-952.
51. Tahawi, Z., Orolinova, N., Joshua, I. G., Bader, M. and Fletcher, E. C. (2001) 'Altered vascular reactivity in arterioles of chronic intermittent hypoxic rats', *J Appl Physiol* (1985), 90(5), pp. 2007-13; discussion 2000.
52. Trzepizur, W., Gaceb, A., Arnaud, C., Ribuot, C., Levy, P., Martinez, M. C., Gagnadoux, F. and Andriantsitohaina, R. (2015) 'Vascular and hepatic impact of short-term intermittent hypoxia in a mouse model of metabolic syndrome', *PLoS One*, 10(5), pp. e0124637.
53. Tsikas, D. (2004) 'Measurement of nitric oxide synthase activity in vivo and in vitro by gas chromatography-mass spectrometry', *Methods Mol Biol*, 279, pp. 81-103.
54. Welch, W. J. (2006) 'Intrarenal oxygen and hypertension', *Clin Exp Pharmacol Physiol*, 33(10), pp. 1002-5.
55. Welch, W. J., Baumgärtl, H., Lübbers, D. and Wilcox, C. S. (2003) 'Renal oxygenation defects in the spontaneously hypertensive rat: role of AT1 receptors', *Kidney Int*, 63(1), pp. 202-8.
56. Welch, W. J., Blau, J., Xie, H., Chabrashvili, T. and Wilcox, C. S. (2005) 'Angiotensin-induced defects in renal oxygenation: role of oxidative stress', *Am J Physiol Heart Circ Physiol*, 288(1), pp. H22-8.
57. Wilcox, C. S. (2005) 'Oxidative stress and nitric oxide deficiency in the kidney: a critical link to hypertension?', *Am J Physiol Regul Integr Comp Physiol*, 289(4), pp. R913-35.
58. Wu, H., Zhou, S., Kong, L., Chen, J., Feng, W., Cai, J., Miao, L. and Tan, Y. (2015) 'Metallothionein deletion exacerbates intermittent hypoxia-induced renal injury in mice', *Toxicol Lett*, 232(2), pp. 340-8.
59. Yokoe, T., Minoguchi, K., Matsuo, H., Oda, N., Minoguchi, H., Yoshino, G., Hirano, T. and Adachi, M. (2003) 'Elevated levels of C-reactive protein and interleukin-6 in patients with obstructive sleep apnea syndrome are decreased by nasal continuous positive airway pressure', *Circulation*, 107(8), pp. 1129-34.
60. Yuan, G., Khan, S. A., Luo, W., Nanduri, J., Semenza, G. L. and Prabhakar, N. R. (2011) 'Hypoxia-inducible factor 1 mediates increased expression of NADPH oxidase-2 in response to intermittent hypoxia', *J Cell Physiol*, 226(11), pp. 2925-33.

779

780

781

782

783

784

785

786

787

788

789 **Figure Legends**

790 **Figure 1**

791 Schematic of the experimental protocol. AIH, acute intermittent hypoxia; CIH, chronic
792 intermittent hypoxia; CPO₂, cortical oxygen tension; MPO₂, medullary oxygen tension; FITC,
793 fluorescein iosthiocyanate.

794 **Figure 2**

795 Mean Arterial Pressure (A), glomerular filtration rate (B), renal blood flow (C) and renal
796 vascular resistance in sham control groups (closed bars) and in animals exposed to intermittent
797 hypoxia (IH, open bars) for 4 hours (acute) or for 8 hours/day for 2 weeks (chronic). * denotes
798 P<0.05 versus corresponding sham value; # denotes P<0.05 versus corresponding exposure
799 group. Bonferroni post hoc test was used for multiple comparisons where appropriate; 2
800 comparisons were performed per family, alpha=0.05

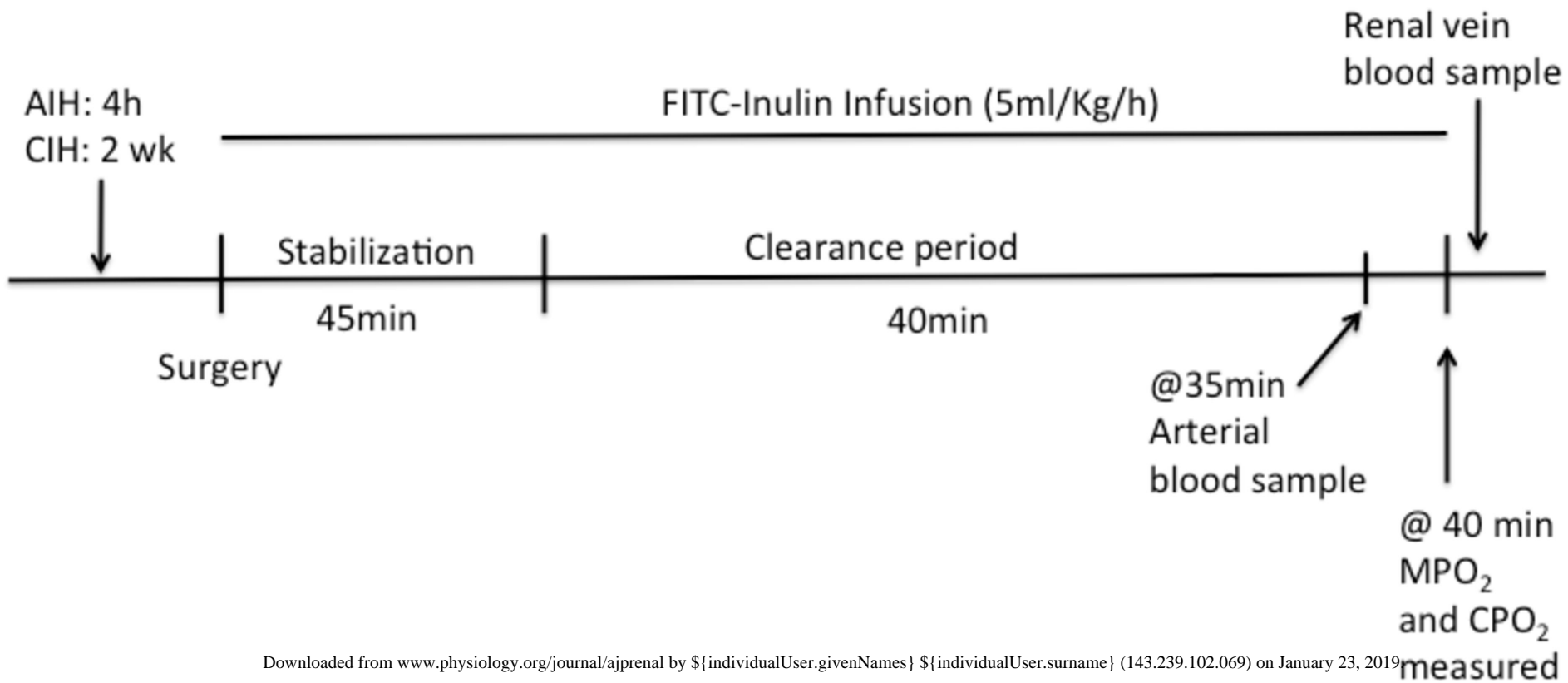
801 **Figure 3**

802 Transported sodium (A), and renal oxygen consumption (B) in sham control groups (closed bars)
803 and in animals exposed to intermittent hypoxia (IH, open bars) for 4 hours (acute) or for 8

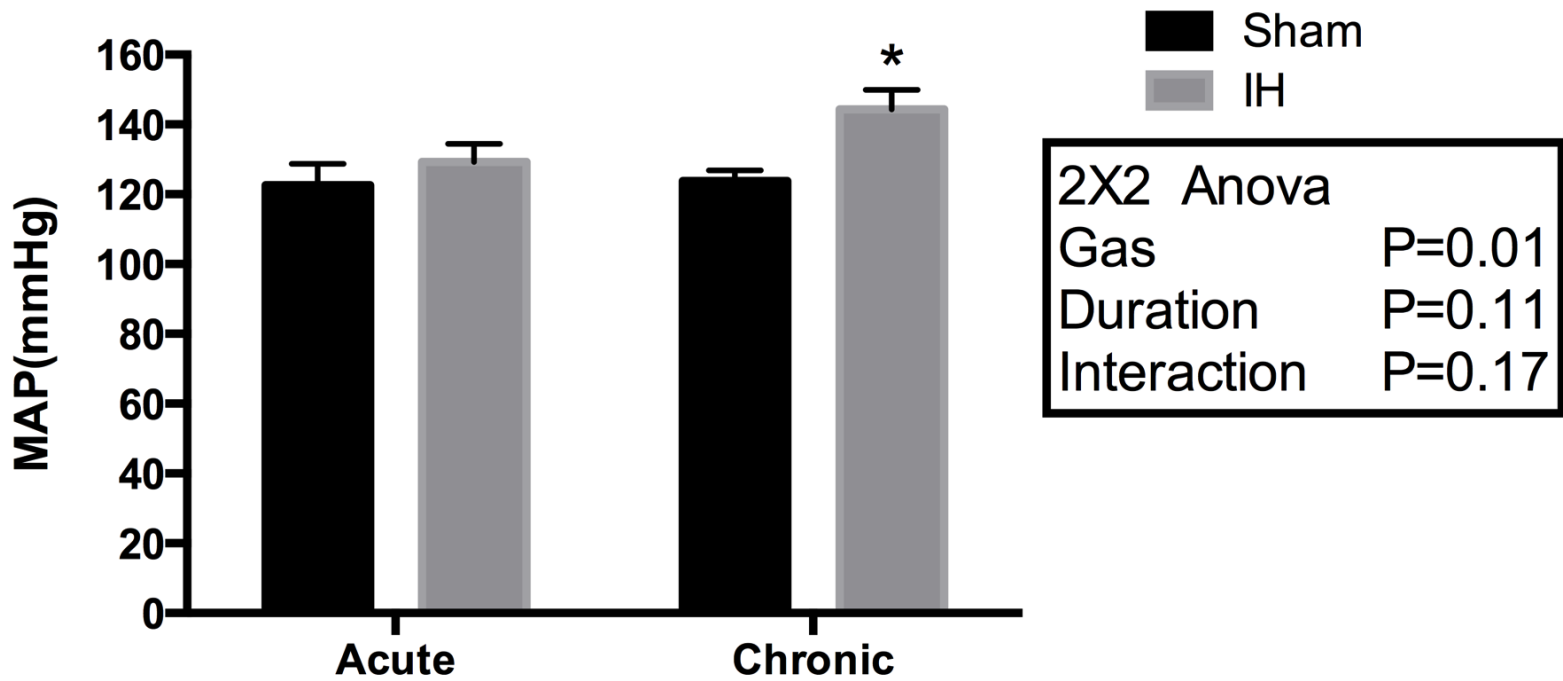
hours/day for 2 weeks (chronic). C shows regression (Deming Model II) analysis examining the relationship between sodium transport and oxygen consumption in the AIH group (green) and the corresponding sham group (pink). D shows regression analysis (Deming Model II) examining the relationship between sodium transport and oxygen consumption in the CIH group (purple) and the corresponding sham (pink). * denotes $P < 0.05$ versus corresponding sham value; # denotes $P < 0.05$ versus corresponding exposure group. Bonferroni post hoc test was used for multiple comparisons where appropriate; 2 comparisons were performed per family, $\alpha = 0.05$

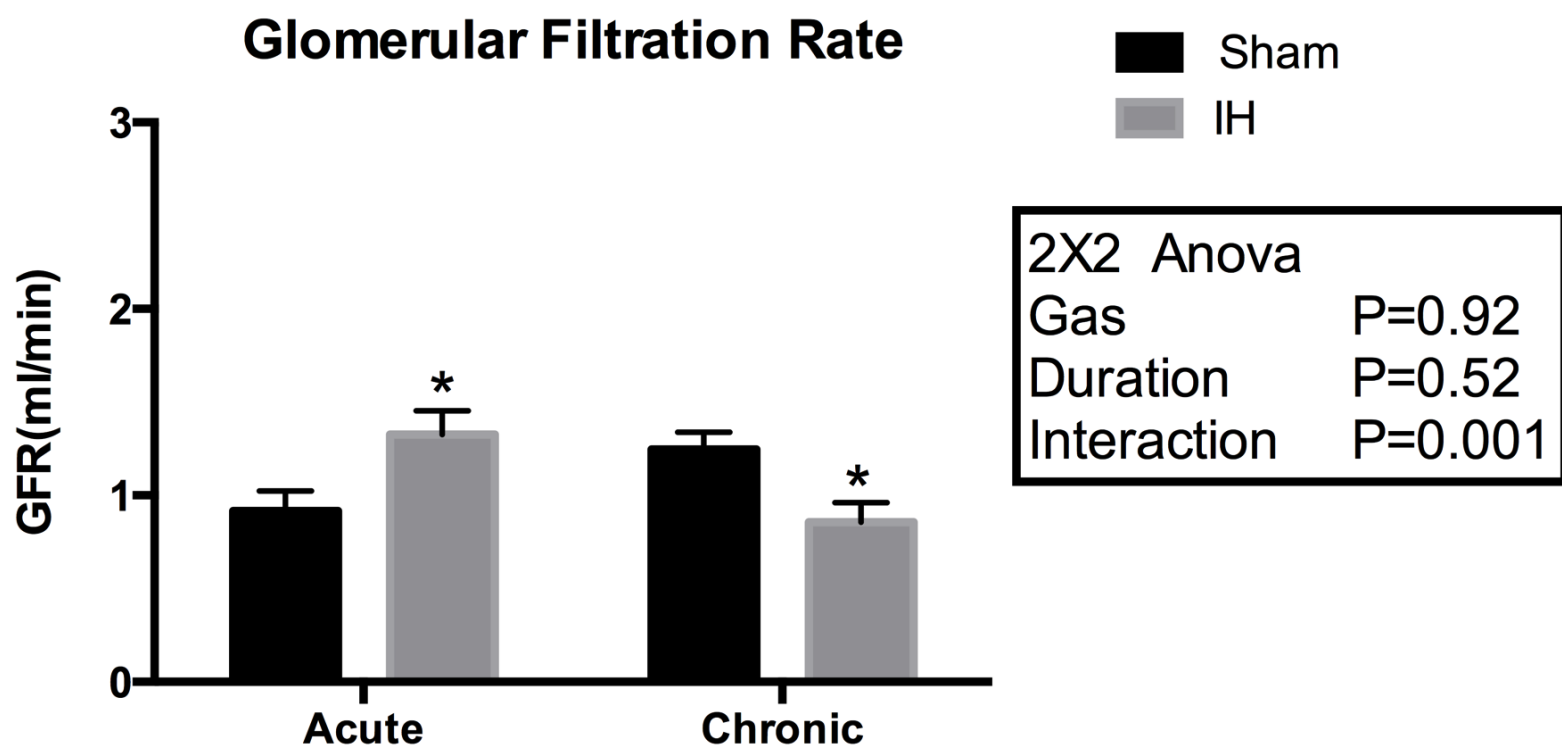
Figure 4

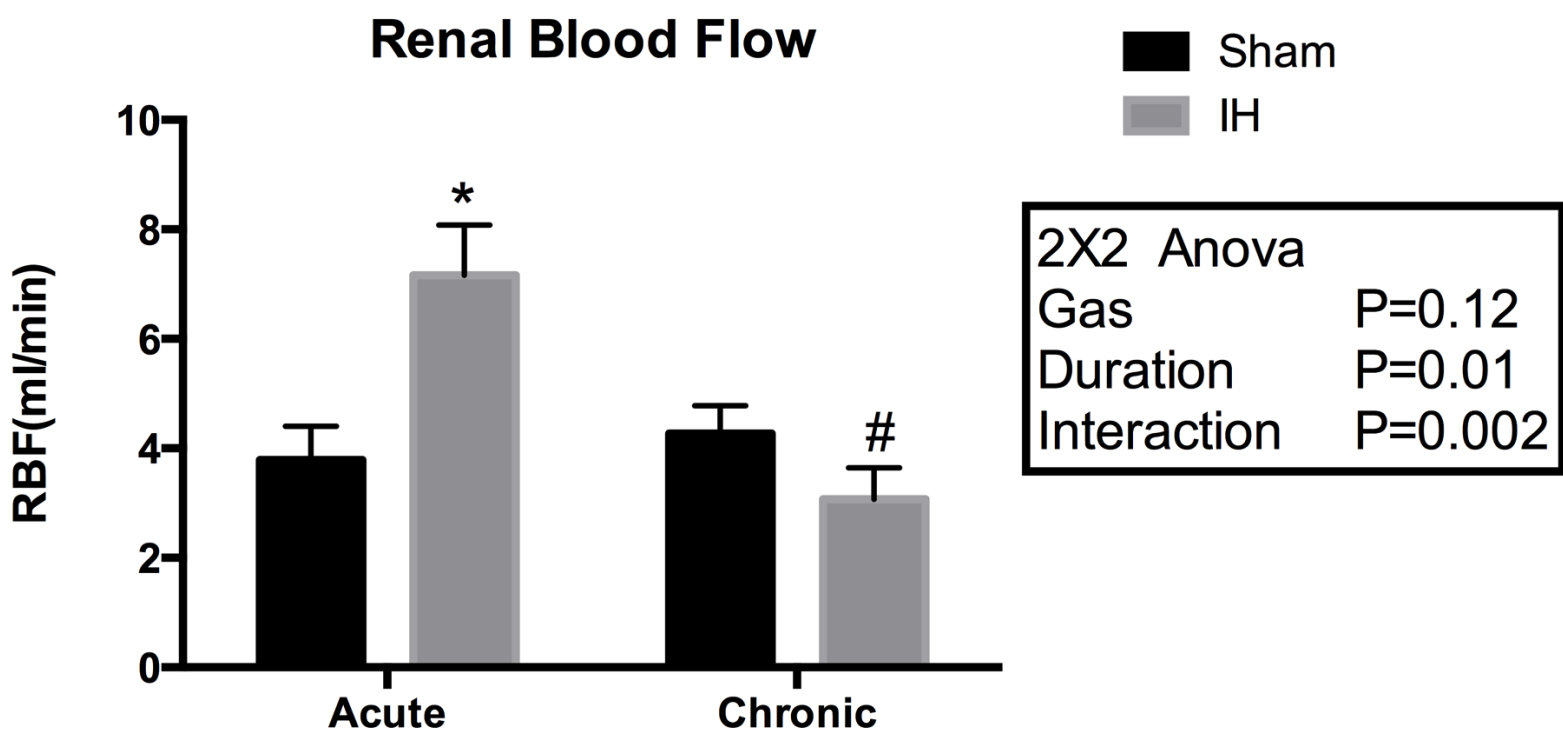
Renal cortex oxygen tension (A), and renal medulla oxygen tension (B) in sham control groups (closed bars) and in animals exposed to intermittent hypoxia (IH, open bars) for 4 hours (acute) or for 8 hours/day for 2 weeks (chronic). * denotes $P < 0.05$ versus corresponding sham value; # denotes $P < 0.05$ versus corresponding exposure group. Bonferroni post hoc test was used for multiple comparisons where appropriate; 2 comparisons were performed per family, $\alpha = 0.05$

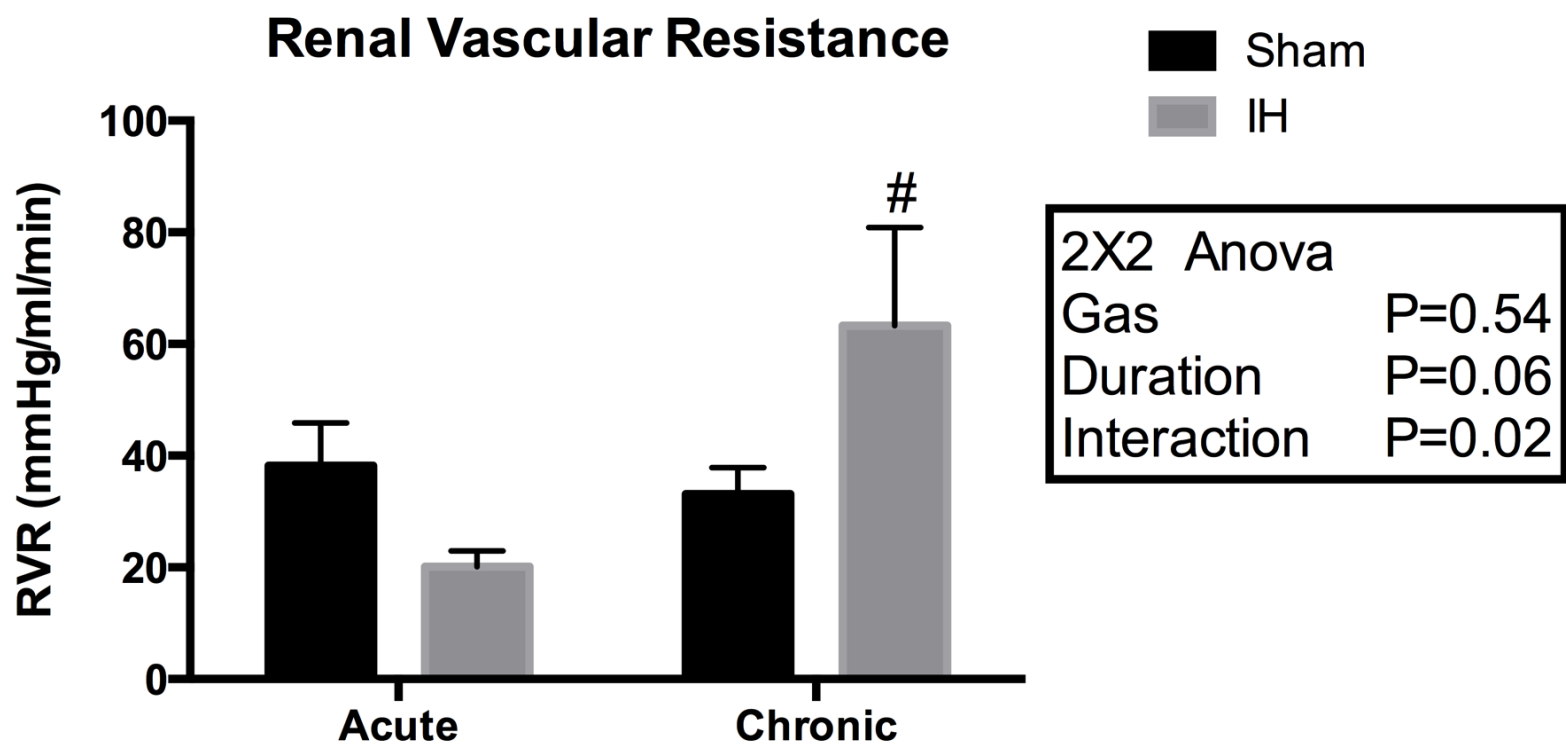


Mean Arterial Pressure

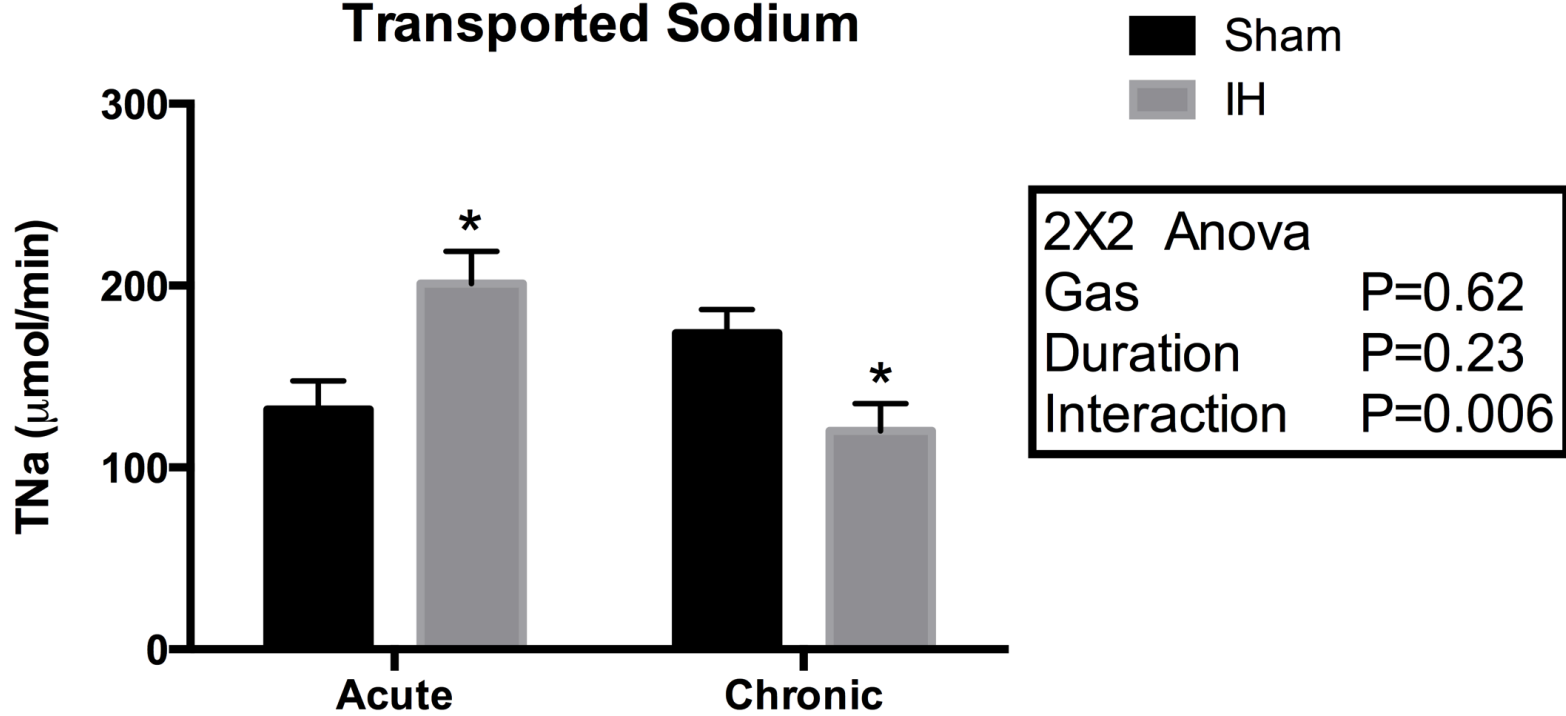


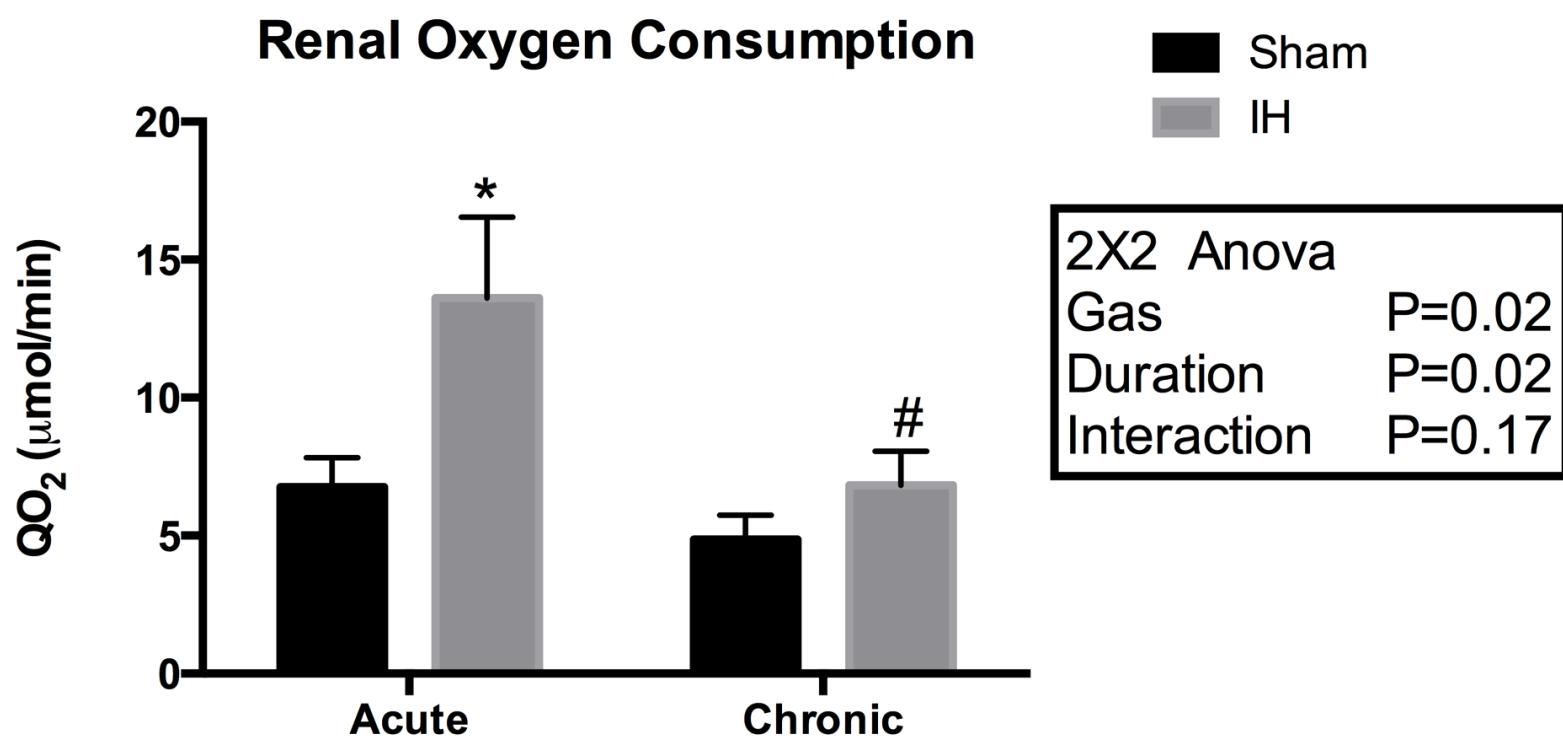


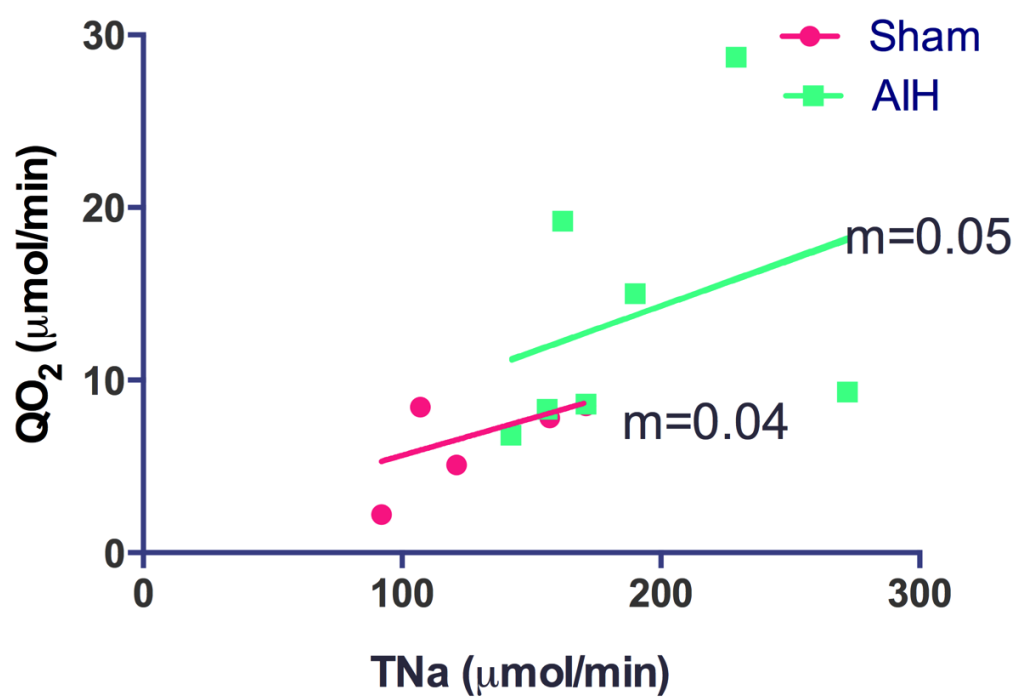




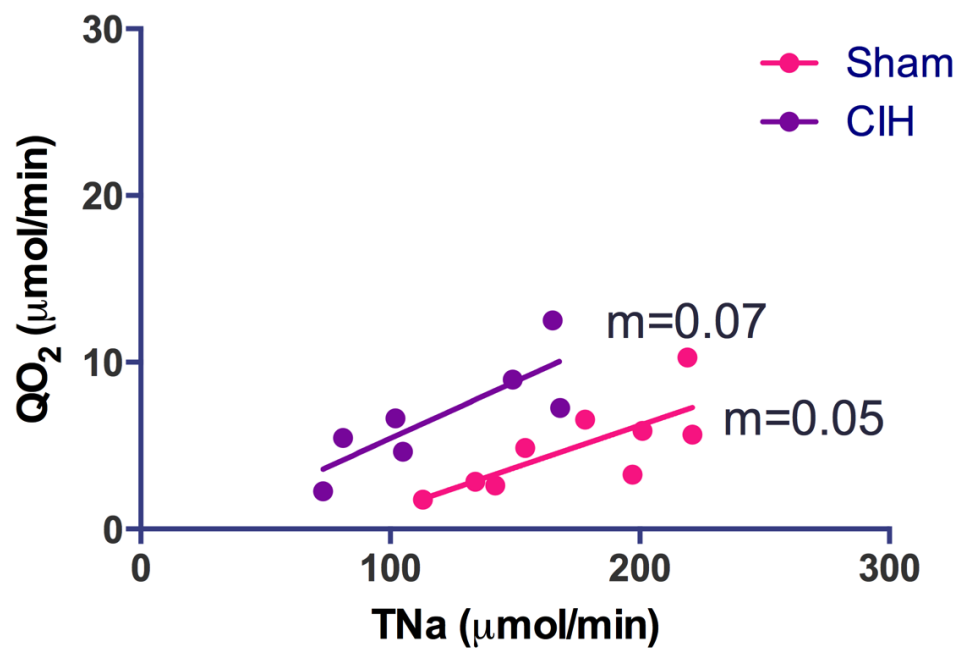
Transported Sodium



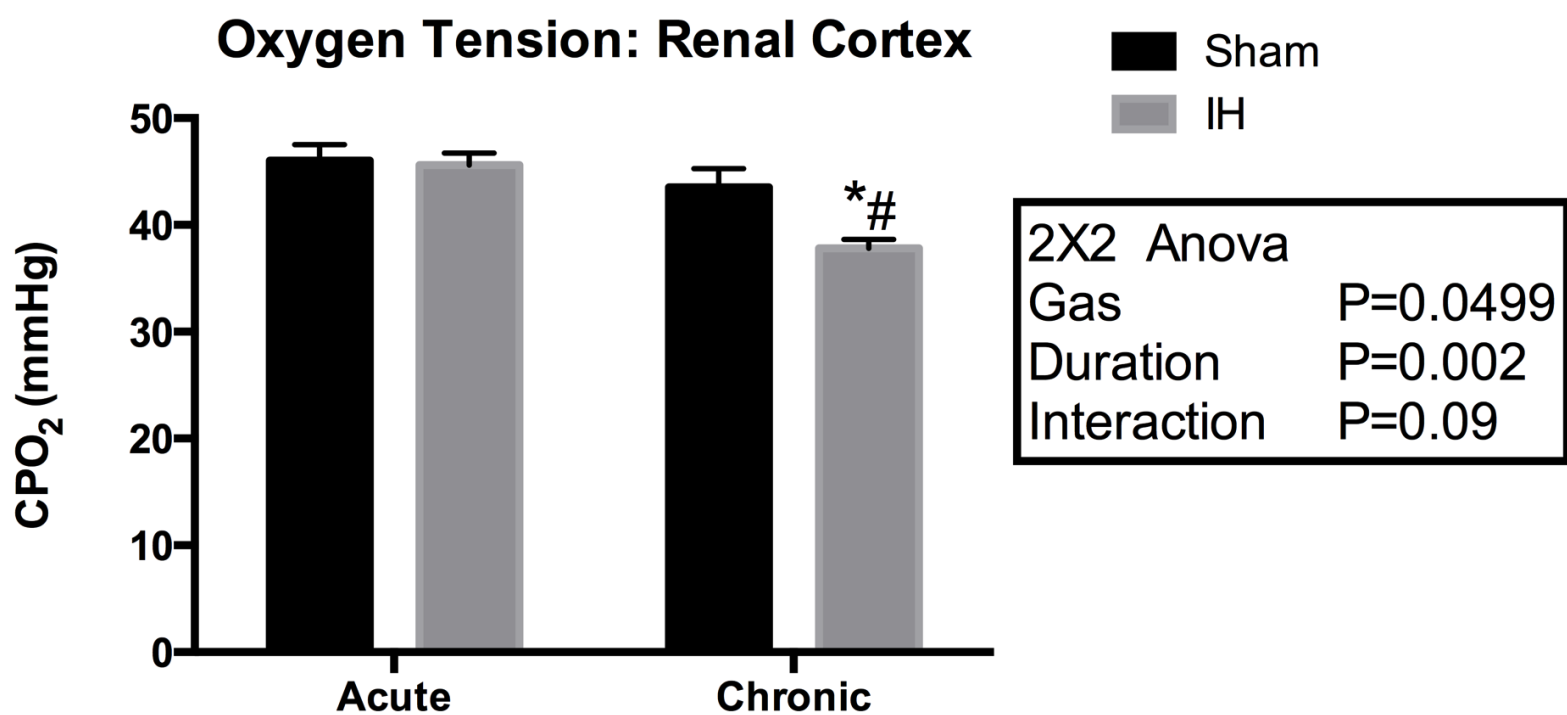




Regression Analysis
slopes: P=0.93
elevation: P=0.41



Regression Analysis
slopes: P=0.31
elevation: P=0.001



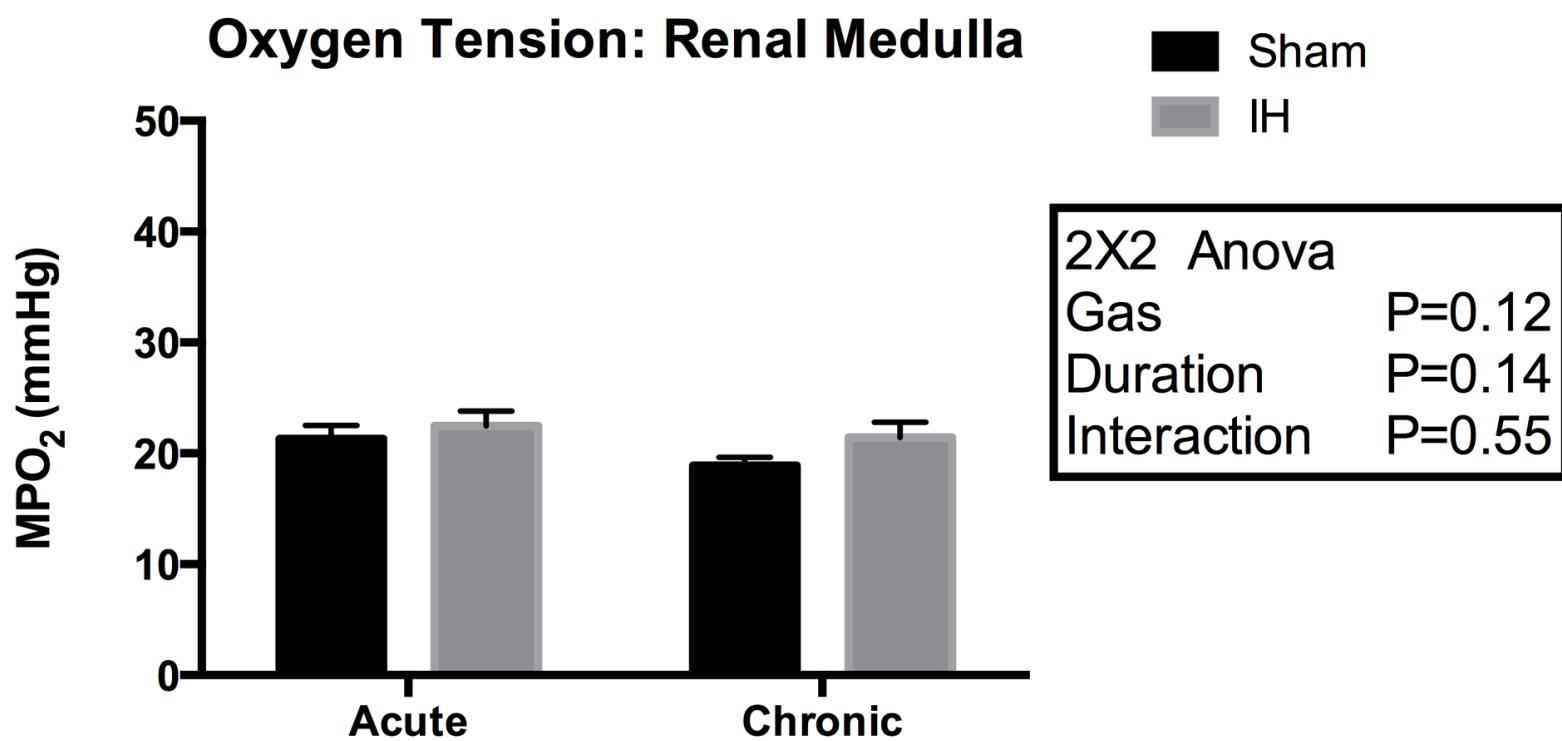


Table1: The effect of AIH and CIH on body weight, arterial blood gases, [Hb] and hematocrit

		Body Weight (g)	[HCO ₃ ⁻] (mmol/L)	pH	PaO ₂ (kPa)	PaCO ₂ (kPa)	[Hb] (g/L)	HCT (%)
Acute	Sham	292±19	23.27±0.61	7.40±0.02	9.82±0.61	5.08±0.25	150.00±4.79	50.33±2.79
	IH	314±20	22.03±0.66	7.40±0.01	10.64±0.31	4.81±0.23	148.43±3.90	52.71±1.23
Chronic	Sham	298±12	25.41±0.50	7.38±0.05	9.05±0.50	5.84±0.28	148.78±5.09	44.56±1.49
	IH	286±16	23.44±0.80	7.43±0.02	11.68±0.28*	4.73±0.01*	176.71±8.82#*	53.00±*2.66
2X2 ANOVA	Gas	<i>P=0.77</i>	<i>P=0.01</i>	<i>P=0.12</i>	<i>P=0.001</i>	<i>P=0.02</i>	<i>P=0.04</i>	<i>P=0.02</i>
	Duration	<i>P=0.48</i>	<i>P=0.03</i>	<i>P=0.70</i>	<i>P=0.77</i>	<i>P=0.24</i>	<i>P=0.03</i>	<i>P=0.20</i>
	Interaction	<i>P=0.32</i>	<i>P=0.84</i>	<i>P=0.10</i>	<i>P=0.06</i>	<i>P=0.15</i>	<i>P=0.02</i>	<i>P=0.15</i>

Data were analyzed using a 2X2 ANOVA and a Bonferroni post -hoc test with 2 multiple comparisons. Data are expressed as mean ± SEM. HCT, hematocrit; Hb, hemoglobin; [HCO₃⁻], Bicarbonate concentration in the arterial blood; PaO₂, arterial oxygen tension; PaCO₂, arterial carbon dioxide tension; IH, intermittent hypoxia; * denotes P<0.05 versus corresponding sham value; # denotes P<0.05 versus corresponding gas group value.

Table 2. Renal excretory effects of AIH and CIH

		Urine Flow ($\mu\text{L}/\text{min}$)	Absolute Sodium Excretion ($\mu\text{mol}/\text{min}$)	Sodium Clearance ($\mu\text{L}/\text{min}$)	Fractional Sodium Excretion (%)	Urinary Protein Excretion ($\mu\text{g}/\text{min}$)	Urinary KIM-1 Excretion (pg/min)
Acute	Sham	2.44 \pm 0.30	0.32 \pm 0.09	2.20 \pm 0.65	0.26 \pm 0.08	68.26 \pm 16.50	---
	IH	6.05 \pm 1.25	0.89 \pm 0.28	6.12 \pm 1.95	0.44 \pm 0.14	68.58 \pm 8.02	---
Chronic	Sham	5.39 \pm 1.27	0.65 \pm 0.24	5.00 \pm 1.72	0.40 \pm 0.14	64.52 \pm 4.47	0.53 \pm 0.12
	IH	3.39 \pm 1.05	0.42 \pm 0.15	2.92 \pm 1.07	0.34 \pm 0.14	132 \pm 41.49	0.93 \pm 0.26
2X2 ANOVA	Gas	<i>P</i> =0.23	<i>P</i> =0.44	<i>P</i> =0.47	<i>P</i> =0.56	<i>P</i> =0.09	
	Duration	<i>P</i> =0.84	<i>P</i> =0.75	<i>P</i> =0.79	<i>P</i> =0.95	<i>P</i> =0.27	
	Interaction	<i>P</i> =0.03	<i>P</i> =0.06	<i>P</i> =0.06	<i>P</i> =0.37	<i>P</i> =0.16	

Data were analyzed using a 2X2 ANOVA and a Bonferroni post –hoc test with 2 multiple comparisons carried out per family. Data are expressed as mean \pm SEM. IH, intermittent hypoxia; KIM-1, Kidney injury marker-1. Urinary KIM-1 excretion data was analyzed using an unpaired t-test comparing sham (n=5) and CIH (n=5); P = 0.2046.

Table 3. Impact of AIH and CIH on systemic and renal NOx and TBARS concentration

		<u>NOx</u>				<u>TBARS</u>		
		Urine (nmol/min)	Plasma (nmol/ml)	Medulla (nmol/mg protein)	Cortex (nmol/mg protein)	Plasma (pmol/ml)	Medulla (pmol/mg protein)	Cortex (pmol/mg protein)
Acute	Sham	1.10\pm0.41	15.92\pm1.37	15.03\pm1.11	18.32\pm1.28	0.35\pm0.14	0.50\pm0.04	0.13\pm0.003
	IH	1.62\pm0.23	11.35\pm0.78*	15.58\pm0.93	11.61\pm1.28*	0.30\pm0.03	0.49\pm0.05	0.13\pm0.01
Chronic	Sham	1.43\pm0.32	16.77\pm2.12	13.99\pm0.73	17.30\pm1.19	0.24\pm0.03	0.61\pm0.08	0.10\pm0.01#
	IH	1.44\pm0.37	9.83\pm1.05*	10.73\pm1.04#	8.14\pm2.00*	0.22\pm0.02	0.43\pm0.06	0.12\pm0.01
2X2 ANOVA	Gas	<i>P=0.46</i>	<i>P=0.0003</i>	<i>P=0.18</i>	<i>P<0.0001</i>	<i>P=0.56</i>	<i>P=0.16</i>	<i>P=0.56</i>
	Duration	<i>P=0.83</i>	<i>P=0.80</i>	<i>P=0.01</i>	<i>P=0.19</i>	<i>P=0.14</i>	<i>P=0.69</i>	<i>P=0.03</i>

<i>Interaction</i>	<i>P=0.44</i>	<i>P=0.35</i>	<i>P=0.06</i>	<i>P=0.47</i>	<i>P=0.80</i>	<i>P=0.20</i>	<i>P=0.18</i>
--------------------	---------------	---------------	---------------	---------------	---------------	---------------	---------------

Data were analyzed using a 2X2 ANOVA and a Bonferroni post -hoc test with 2 multiple comparisons carried out per family. Data are expressed as mean \pm SEM. IH, intermittent hypoxia; NO_x, Nitrate/Nitrite metabolites; TBARS, Thiobarbituric acid reactive substances. * denotes P<0.05 versus corresponding sham value; # denotes P<0.05 versus corresponding gas group value.

Table 4. Impact of AIH and CIH on inflammatory cytokine profiles in the renal cortex.

		IFN- γ (pg/mg protein)	IL-1 β (pg/mg protein)	IL-6 (pg/mg protein)	KC/GRO (pg/mg protein)	IL-10 (pg/mg protein)	TNF- α (pg/mg protein)
Acute	Sham	1.19 \pm 0.23	23.21 \pm 2.71	93.48 \pm 23.53	63.40 \pm 5.42	4.82 \pm 0.88	2.00 \pm 0.18
	IH	3.94 \pm 1.11	35.34 \pm 8.67	229.72 \pm 93.42	66.27 \pm 15.28	3.40 \pm 0.89	3.35 \pm 1.36
Chronic	Sham	2.70 \pm 1.15	35.61 \pm 5.27	117.24 \pm 24.66	62.26 \pm 8.38	3.03 \pm 0.68	2.36 \pm 0.46
	IH	4.63 \pm 1.31	31.83 \pm 4.43	62.41 \pm 20.10	28.96 \pm 7.38	3.11 \pm 0.84	1.48 \pm 0.46
2X2 ANOVA	Gas	<i>P</i> =0.0455	<i>P</i> =0.47	<i>P</i> =0.55	<i>P</i> =0.21	<i>P</i> =0.65	<i>P</i> =0.77
	Duration	<i>P</i> =0.31	<i>P</i> =0.45	<i>P</i> =0.18	<i>P</i> =0.11	<i>P</i> =0.38	<i>P</i> =0.39
	Interaction	<i>P</i> =0.67	<i>P</i> =0.20	<i>P</i> =0.13	<i>P</i> =0.09	<i>P</i> =0.58	<i>P</i> =0.20

Data were analyzed using a 2X2 ANOVA and a Bonferroni post -hoc test with 2 multiple comparisons carried out per family. Data are

expressed as mean \pm SEM. IH, Intermittent hypoxia; IFN- γ , Interferon- γ ; IL-1 β , Interleukin-1 β ; IL-6, Interleukin-6; KC/GRO, chemokine/growth related oncogene; IL-10, interleukin-10; TNF- α , Tumor necrosis factor- α .

Table 5 Impact of AIH and CIH on renal gene expression

		NOS-1	NOS-3	VEGF	NOX 4	HO-1	HIF-1 α	NF- κ B
Groups	Pooled Sham	1.05\pm0.13	1.11\pm0.16	1.01\pm0.05	1.01\pm0.16	1.21\pm0.28	0.97\pm0.13	0.92\pm0.08
	AIH	1.12\pm0.15	1.11\pm0.07	1.09\pm0.07	1.03\pm0.14	0.72\pm0.22	1.01\pm0.11	0.88\pm0.17
	CIH	1.48\pm0.22	1.50\pm0.14	1.24\pm0.11	1.44\pm0.18	0.84\pm0.21	1.34\pm0.27	1.73\pm0.50
ONE WAY ANOVA	P-Value	0.19	0.09	0.13	0.14	0.34	0.33	0.08

Data were analyzed using a one-way ANOVA with a Bonferroni pot-hoc test with 2 multiple comparisons carried out per family. mRNA levels are expressed as fold change relative to the HPRT reference gene. Data are expressed as mean \pm SEM. AIH, acute intermittent hypoxia; CIH, chronic intermittent hypoxia; NOS-1; neuronal nitric oxide synthase; NOS-3 endothelial nitric oxide synthase; VEGF vascular endothelial growth factor; NOX 4 NADPH (nicotinamide adenine dinucleotide phosphate hydrogen) oxidase 4; HO-1, haemoxygenase 1; HIF, hypoxia inducible factor; NF- κ B, nuclear factor kappa B.